

AD
NOL-TR-1365

ION AND ELECTRON DISTRIBUTIONS IN THE
BOUNDARY LAYER OF HYPERSONIC VEHICLES
FOR CHEMICAL NON-EQUILIBRIUM FLOW

Part I

AERODYNAMICS AND NUMERICAL RESULTS

by

Irvin Fedin

November 1971

NATIONAL TECHNICAL
INFORMATION SERVICE

U.S. ARMY MATERIEL COMMAND

HARRY DIAMOND LABORATORIES

WASHINGTON, D.C. 20435

APPROVED FOR PUBLIC RELEASE DISTRIBUTION

Unclassified

Security Classification

DOCUMENT CONTROL DATA - R & D		
(Security classification of title, body of abstract and indexing annotation must be entered when the overall report is classified)		
1. ORIGINATING ACTIVITY (Corporate author)		2a. REPORT SECURITY CLASSIFICATION
Harry Diamond Laboratories Washington, D. C. 20438		Unclassified
		2b. GROUP
3. REPORT TITLE		
Ion and Electron Distributions in the Boundary Layer of Hypersonic Vehicles for Chemical Non-Equilibrium Flow Part I - Aerodynamics and Numerical Results		
4. DESCRIPTIVE NOTES (Type of report and inclusive dates)		
5. AUTHOR(S) (First name, middle initial, last name)		
Irvin Pollin		
6. REPORT DATE	7a. TOTAL NO. OF PAGES	7b. NO. OF REFS
November 1971	36	32
8a. CONTRACT OR GRANT NO.	8b. ORIGINATOR'S REPORT NUMBER(S)	
9. PROJECT NO DA-1T-061101A91A	HDL-TR-1565	
AMCMS Code: 501A.11.84400	9b. OTHER REPORT NO(S) (Any other numbers that may be assigned this report)	
HDL Proj: ILIR15		
10. DISTRIBUTION STATEMENT		
Approved for public release; distribution unlimited.		
11. SUPPLEMENTARY NOTES	12. SPONSORING MILITARY ACTIVITY	
	U. S. Army Materiel Command	
13. ABSTRACT		
<p>Flows over non-ablating hypersonic vehicles are considered when all electrons are produced by aerodynamic heating in the boundary layer. Detailed calculations of the ion and electron distributions are presented for a vehicle with a conical nose and a semivertex angle of 10 deg, for Mach numbers 8 and 10 at sea level. Except for a small region at the nose, the boundary layer is turbulent. Diffusion of electrons with respect to the ions and neutrals is considered and ambipolar diffusion is found to occur across most of the boundary layer only at large ion-electron densities.</p>		

DD FORM 1473

REPLACES DD FORM 1473, 1 JAN 64, WHICH IS OBSOLETE FOR ARMY USE.

Unclassified

Security Classification

35

DATE	TIME	BY
REMARKS		

The findings in this report are not to be construed as an official Department of the Army position unless so designated by other authorized documents.

Citation of manufacturers' or trade names does not constitute an official endorsement or approval of the use thereof.

Destroy this report when it is no longer needed. Do not return it to the originator.

14 KEY WORDS	LINK A		LINK B		LINK C	
	ROLE	WT	ROLE	WT	ROLE	WT
Ionized flow	8	3				
Plasma	8	3				
Hypersonic vehicles	8	3				
Electron density distribution	8	3				
Non-equilibrium chemical flow	8	3				

AD

DA-1T-061101A91A
AMCMS Code: 501A.11.84400
HDL Proj: ILR15

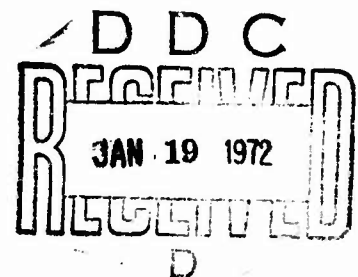
HDL-TR-1565

**ION AND ELECTRON DISTRIBUTIONS IN THE
BOUNDARY LAYER OF HYPERSONIC VEHICLES
FOR CHEMICAL NON-EQUILIBRIUM FLOW**

**Part I
AERODYNAMICS AND NUMERICAL RESULTS**

**by
Irvin Pollin**

November 1971



U.S. ARMY MATERIEL COMMAND,
HARRY DIAMOND LABORATORIES
WASHINGTON, D.C. 20438

APPROVED FOR PUBLIC RELEASE; DISTRIBUTION UNLIMITED.

ABSTRACT

Flows over non-ablating hypersonic vehicles are considered when all electrons are produced by aerodynamic heating in the boundary layer. Detailed calculations of the ion and electron distributions are presented for a vehicle with a conical nose and a semivertex angle of 10 deg, for Mach numbers 8 and 10 at sea level. Except for a small region at the nose, the boundary layer is turbulent. Diffusion of electrons with respect to the ions and neutrals is considered and ambipolar diffusion is found to occur across most of the boundary layer only at large ion-electron densities.

CONTENTS

ABSTRACT	3
1. INTRODUCTION.....	7
2. NEUTRAL GAS FLOW AND THERMODYNAMIC PROPERTIES.....	8
3. GOVERNING EQUATIONS FOR THE CHARGED PARTICLES.....	13
4. BOUNDARY CONDITIONS.....	17
5. NUMERICAL CALCULATIONS FOR THE ION AND ELECTRON FLOW IN THE BOUNDARY LAYER.....	18
6. CONCLUSIONS.....	21
7. LIST OF SYMBOLS.....	23

TABLES

I. Mach number 8.....	25
II. Mach number 10.....	28

FIGURES

1a. Boundary layer parameters \bar{D} , P and T - Mach number 8....	14
1b. Boundary layer parameters \bar{D} , P and T - Mach number 10....	14
2a. Ion and electron densities at $\eta = 0.01, 0.1$ and 0.5 Mach number 8.....	19
2b. Ion and electron densities at $\eta = 0.01, 0.1$, and 0.5 Mach number 10.....	19
3a. Electric field and potential at $X = 100\text{cm}$ - Mach number 8.....	19
3b. Ion and electron densities at $X = 5.62$ and 100cm - Mach number 8.....	19
3c. Electric field and potential at $X = 5.62$ and 100cm - Mach number 10.....	20
3d. Ion and electron densities at $X = 5.62$ and 100cm - Mach number 10.....	20

1. INTRODUCTION

The accuracy with which a hypersonic vehicle receiving microwave radiation through a dielectric window can track a target is affected by electrons produced by aerodynamic heating in the boundary layer of the tracking vehicle. The plasma distorts an incoming signal by changing its propagation velocity through the plasma, refracting it at the plasma radome interface, and causing additional changes in the passage of the signal within the radome itself. Accordingly, wherever the electron number density exceeds $10^8/\text{cm}^3$, the calculation of boresight error requires a description of the electron distribution.¹

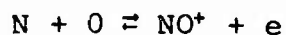
In the present case, detailed calculations for the ion and electron distributions are given for a tracking vehicle having the form of a 10-degree semivertex cone flying at zero angle of incidence, sea level, and Mach numbers 8 and 10. We assume that the vehicle is subjected to intense aerodynamic heating for a short time duration, so that no ablation occurs and the vehicle shape is unaltered. Hence, with a pointed or slightly rounded non-ablating nose, the electron production occurs entirely within a small fraction of the hot boundary layer adjacent to the vehicle surface. For the above conditions, the boundary layer is turbulent everywhere except for a very small region near the nose.

The random translational energy of the electrons is at most 0.4 electron-volt, and those electrons are subject to large accelerations by small electric fields. Thus, the electron production (as affected by recombination) as well as the distribution are sensitive to the small electric fields produced by charge separation, caused by the faster diffusion of electrons relative to ions from the region of higher ionization production. The electric field sets up a conduction current which tends toward ambipolar diffusion with increasing levels of ionization.

For the above flows, the enthalpy distribution is decoupled from the ionization, since the ionization enthalpy is insignificant in comparison with the local enthalpy. The ion mass fraction nowhere exceeds 10^{-4} . Accordingly, all electrons are produced through the reaction²

¹ Private communications, T.B.A. Senior, Univ. of Michigan, and G. Tricoles, General Dynamics-Electronics, San Diego, California, March 1971.

² J. Hilsenrath, and M. Klein, Tables of Thermodynamic Properties of Air in Chemical Equilibrium Including Second Virial Corrections from 1500°K to 15,000°K, Arnold Engineering Development Center, AEDC-TR-65-58, March 1965.



(1)

Moreover, the effect of Coulomb forces on collisions between neutral particles and between ions and neutral particles is negligible. Consequently, the neutral gas viscosity and ion diffusion coefficients are not affected by the electric field.⁵

In the present calculations, we account for the turbulent boundary layer by assuming a power-law velocity distribution for the neutral gas and an associated iso-energetic enthalpy boundary layer. This procedure allows for the complete determination of the neutral gas flow. Binary and turbulent eddy diffusion coefficients are included in the calculation of the ion-electron drift velocities. The boundary layer equations governing the electron and ion distributions are then solved exactly for dissociation equilibrium and ionization non-equilibrium.

The uncertainties in the boundary conditions, such as body temperature and body electric potential, justify use of this approximate method of solution. These conditions are usually known only to within a range of values that can yield variations in ion and electron distributions easily exceeding the error introduced by our method of solution. In addition, the effect on the ion and electron distributions by the neutral particle velocity distribution and boundary layer thickness can be readily obtained by our procedure. For prescribed boundary conditions, the present procedure permits a readily obtainable approximate evaluation of the plasma distribution for a wide range of body geometries and flow conditions.

2. NEUTRAL GAS FLOW AND THERMODYNAMIC PROPERTIES

For the cone of semivertex angle 10 deg considered here, significant shock wave ionization does not occur. High temperature and associated ionization, say $10^8/\text{cm}^3$ or larger, occur only within a small fraction of the boundary layer. As previously stated, all ions and electrons are produced by the reaction given by equation (1). Assuming ion formation from N_2 and O_2 , approximately 10 ev per ion are required. The energy required to form

⁵ I. Pollin, The Stagnation-Point Langmuir Probe in a Shock Tube-Theory and Measurements, Harry Diamond Labs, HDL TR-1103, 28 June 1963.

$10^{14}/\text{cm}^3$ electrons, which exceeds the equilibrium ion density formed on the above body at Mach number 10 and sea level, is $1.6 (10^{-4})$ joule/ cm^3 . This energy is insignificant in comparison with the Mach number 10 sea level free stream total enthalpy of 7.5 joule/ cm^3 . Thus, the neutral gas enthalpy is decoupled from the ionization.

We assume the boundary layer neutral gas velocity profile corresponding to turbulent flow to be of the form⁴⁻⁸

$$u = u_{\delta} \eta^{\frac{1}{m}} \quad (2)$$

The extent of the laminar sublayer adjacent to the vehicle surface is about 1 percent of the total boundary layer thickness. Except for this displacement, the turbulent layer is unaffected by its presence, since only a small fraction of the momentum lies in the sublayer.^{9,10} The velocity power law given by equation (2) is representative of a large class of fully developed turbulent boundary

-
- ⁴ R.K.Lobb, E.M.Winkler, and J.Persh, Experimental Investigation of Turbulent Boundary Layers in Hypersonic Flow, J.Aeronaut.Sci.22, 1-9-50 (1955).
 - ⁵ D.M.Bushnell, and I.F.Beckwith, Calculation of Hypersonic Turbulent Boundary Layers and Comparison With Experimental Data, AIAA Paper No. 69-684, June 16-18, 1969.
 - ⁶ H.L.Dryden, Transition from Laminar to Turbulent Flow, High Speed Aerodynamics and Jet Propulsion, Vol.V: Turbulent Flows and Heat Transfer, Princeton Univ. Press, 1959, Edited by C.C.Lin.
 - ⁷ C.M.Jackson, and R.S.Smith, A Method for Determining the Total Drag of a Pointed Body of Revolution in Supersonic Flow with Turbulent Boundary Layer, National Aeronautics and Space, NASA TN D-5046, March 1969.
 - ⁸ D.L.Brott, W.J.Yanta, R.L.Voisinet, and R.L.Lee. An Experimental Investigation of the Compressible Turbulent Boundary Layer with a Favorable Pressure Gradient, AIAA Paper No. 69-685, June 16-18, 1969.
 - ⁹ Ibid.
 - ¹⁰ W.D.Hayes and R.F.Probstein, Hypersonic Flow Theory, pp 327-339, Academic Press, Inc., 1959.

layer flows at high and low Mach number, and therefore provides an adequate basis for determining the neutral gas velocity. The appropriate value of m appears to be between 6 and 8; $m = 8$ was used in the present calculations⁹⁻¹². As previously stated, the effect on the electron distribution caused by variation of m within this range is small in comparison with that produced by other uncertainties, such as the value of the vehicle temperature.

The boundary layer thickness $\delta = \delta(x)$ (defined as the distance measured normal to the wall where the velocity is 0.99 of the local free stream value) depends on such factors as the wall temperature, vehicle contour and flight conditions.¹⁰⁻¹² For example, at high Mach numbers, the effect of insulating the body is an increase in the boundary layer temperature and thereby, a reduction in the density and an increase of the boundary layer thickness. Usually, δ increases as the flow proceeds downstream, and thereby new fluid continually enters the boundary layer and is heated.

For fully developed turbulent boundary layer flow, at Mach numbers 1.8 and 4.25 the boundary layer thickness on an axisymmetric cone with the semivertex angle of $12\frac{1}{2}$ deg was everywhere found to be less than 10 percent of the local cone radius at all angles of incidence up to at least 15 deg. At the latter angle, the value of δ on the leeward side was found to be a factor of 5 larger than that on the windward side at the same downstream station.¹³ The large variation of boundary layer thickness is brought about primarily by the circumferential pressure gradient. A favorable pressure gradient (pressure decreasing in the direction of the flow) always tends to reduce the rate of increase in δ ; the opposite is also true. Thus, at a given axial station, the boundary layer thickness can circumferentially vary by a factor of 2 at 2 deg angle of incidence and by a factor more than 3 at 5 deg.¹³ Consequently, unless the flow conditions and body geometry are known, only approximate values of $\delta = \delta(x)$ can be prescribed.

¹¹ R.K.Lobb, E.M.Winkler, and J.Persh, Experimental Investigation of Turbulent Boundary Layers in Hypersonic Flow, J.Aeronau.Sci. 22, 1-9-50, 1955.

¹² D.M.Bushnell, and I.F.Beckwith, Calculation of Hypersonic Turbulent Boundary Layers and Comparison with Experimental Data, AIAA Paper No. 69-684, June 16-18, 1969.

¹³ W.J.Rainbird, Turbulent Boundary Layer Growth and Separation on a Yawed $12\frac{1}{2}^\circ$ Cone at Mach Numbers 1.8 and 4.25. AIAA Paper No. 68-98, Jan 22-24, 1968.

The peak boundary layer electron density is reduced by diffusion, moreover, the ionization process is comparatively slow, so that equilibrium values of peak electron density are nowhere attained. Therefore, in an iso-energetic boundary layer, this means that the peak electron density will tend to increase with increasing δ . For moderate angles of incidence a reasonable estimate of δ is given by flat plate theory and Rainbird's data,¹² from which we deduce

$$\delta = bx^a \quad (3)$$

with $a = 0.8$. The effect of δ on the electron distribution can be calculated by adjusting b over the range $0.02 > b \geq 0.002$. The smaller value of δ is associated with low altitudes, the windward side of the vehicle, etc. In the calculations, $b = 0.02$ was used.

The pressure distribution across the boundary layer is given by $\partial p / \partial y = 0$. For cones, in the inviscid region $p = \text{constant}$ along a conical generator. Hence, $p = \text{constant}$ throughout the boundary layer for conical vehicles. Inside the boundary layer,

$$\rho = p/RTZ \quad (4)$$

For a fully developed turbulent flow in dissociative equilibrium on a conical body, the boundary layer enthalpy distribution is given by the Crocco relation

$$H = h_u + (H_\delta - h_b) \frac{u}{u_\delta},$$

when the laminar and turbulent Prandtl and Lewis numbers are unity.^{14,15} For $H = h_b$, we obtain an isoenergetic boundary layer, so that

$$h = h_b - \frac{u^2}{2} \quad (5)$$

Throughout the boundary layer, $v \ll u$; consequently, the v term is not included in the calculation for h .

¹⁴ W.D.Hayes and R.F.Probstein, Hypersonic Flow Theory, pp 327-339, Academic Press Inc., 1959.

¹⁵ L.H.Back and R.F.Cuffel, Relationship Between Temperature and Velocity Profiles In A Turbulent Boundary Layer Along A Supersonic Nozzle With Heat Transfer. AIAA Journal, Nov., 1970.

Actually, the equilibrium value of h_p is limited by the recovery factor, which has the value 0.90 for turbulent boundary layers. The value of h given by (5) is everywhere at most 10 percent larger than that obtained by assuming $h_p = .90 H_e$ in the Crocco relation. The resulting difference in electron distribution is well within the difference corresponding to the uncertainty in describing actual flight conditions. The effect of assuming an isocenergetic boundary layer is equivalent to attaining a given peak electron density at a slightly lower Mach number with a slightly different electron distribution.

With the use of equation (2), the energy equation becomes

$$\int_{\delta}^{\eta} dh = \frac{u_{\delta}^2}{2} (1 - \eta^{-\frac{2}{m}}) \quad (6)$$

In equation (6), the recovery enthalpy is reached at $\eta = (0.1)^{\frac{m}{2}}$. The enthalpy then was assumed constant for $(0.1)^{\frac{m}{2}} \leq \eta < 0$.

The flow thermodynamic properties at $y = \delta$ were calculated for the conical flow at zero angle of incidence with the help of the Sims' tables.¹⁶ The formation of equilibrium values of dissociated N and O takes place within several hundred collisions.^{17,18,19} The largest mean free path in the present calculations is of the order 10^{-5} cm. Thus, the boundary layer will be in chemical equilibrium with respect to the dissociated N and O. Since $T = T(\eta)$ and $p = \text{constant}$, the N and O distributions are functions of η only.

¹⁶ J.L.Sims, Tables for Supersonic Flow Around Right Circular Cones at Zero Angle of Attack, National Aeronautics and Space Administration, NASA SP-3004, 1964.

¹⁷ M.H.Bloom and M.H.Steiger, Inviscid Flow with Non-equilibrium Molecular Dissociation for Pressure Distributions Encountered in Hypersonic Flight, Journal of the Aero/Space Sciences, Vol.27, No.11, November 1960.

¹⁸ K.L.Wray, Chemical Kinetics of High Temperature Air International Hypersonics Conference, M.I.T., Cambridge, Mass., Aug. 16-18, 1961.

¹⁹ S.C.Lin, and J.D.Teare, Rate of Ionization Behind Shock Waves in Air, II. Theoretical Interpretation, Avco Research Report 115, Sept. 1962.

Moreover, because the ionization enthalpy is small in comparison with the free stream enthalpy, we may assume dissociative equilibrium in the boundary layer, and thereby $h = h(\rho, T)$. Then, with the use of equations (4) and (6), the thermodynamic properties were found for $y < \delta$ using the tables of Hilsenrath and Klein.²⁰ In every case, T_δ is so small that dissociation is zero and $\bar{Z} = 1$ at $y = \delta$. Within the boundary layer, $Z = Z(\rho, T)$.

The component of the neutral gas velocity normal to the conical surface, v , is obtained from the mass conservation equation for axisymmetrical flow,

$$(\rho u r)_x + (\rho v r)_y = 0 \quad (7)$$

Since ρ and u are known functions of η , and r and δ are known functions of x , the solution of equation (7) becomes

$$v = \frac{a u_\delta \delta \eta^{\frac{m+1}{m}}}{x} - [1+a] \frac{\delta u_\delta P}{x} \int_0^\eta \frac{\eta^{\frac{1}{m}}}{P} d\eta \quad (8)$$

Since $r \ll x$ and $\delta \ll x$, by equations (2) and (8), $v \ll u$; therefore, as previously noted, the effect of v on h is everywhere negligible. However, v has significance in the computation of the ion and electron velocities and thereby on their corresponding density distributions.

3. GOVERNING EQUATIONS FOR THE CHARGED PARTICLES

For axisymmetric flow, the conservation equations for the ions and electrons are

$$\rho u s_x^+ + \rho v s_y^+ = (\rho D s_y^{++} + \rho D_T s_y^+) + (\rho K s_y^{++}) + \frac{\dot{W}^+}{c_e} \quad (9)$$

$$\rho u \bar{s}_x + \rho v \bar{s}_y = (\rho \bar{D} \bar{s}_y + \rho D_T \bar{s}_y) - (\rho \bar{K} \bar{s}_y) + \frac{\bar{W}}{\bar{c}_e} \quad (10)$$

where $\frac{\dot{W}^+}{c_e} = \frac{\bar{W}}{\bar{c}_e} = c_e$ and

$$\frac{\dot{W}^+}{M} = \frac{\bar{W}}{\bar{M}} = \frac{dn}{dt} = K_f \langle N \rangle \langle O \rangle - K_r \dot{n} \bar{n}, \quad (11)$$

²⁰ J. Hilsenrath and M. Klein, Tables of Thermodynamic Properties of Air in Chemical Equilibrium Including Second Virial Corrections from 1500°K to 15,000°K, Arnold Engineering Development Center, AEDC-TR-65-58, March 1965.

and the formation and recombination rate constants are given as^{21,22,23,24}

$$K_f = 5(10^{-11})T^{-3.5} \exp(-32,500/T) \text{ and} \quad (12)$$

$$K_r = 3(10^{-3})T^{-1.5} \text{ cm}^3/\text{ion-sec},$$

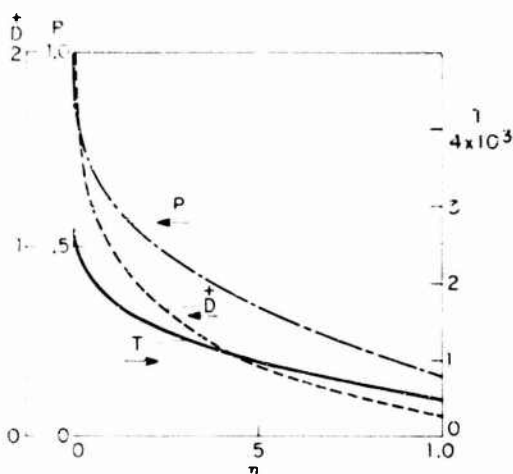


Fig. 1(a) Boundary layer parameters
D, P and T - mach number 8

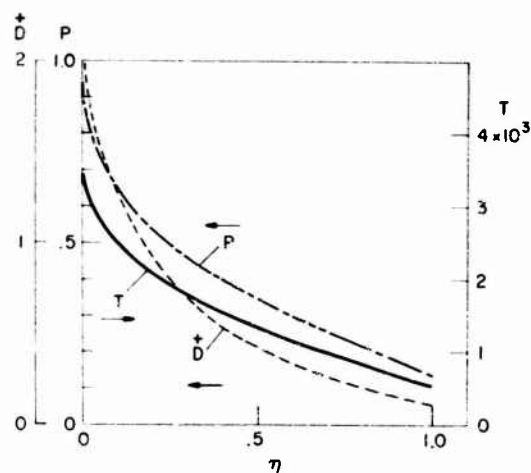


Fig. 1(b) Boundary layer parameters
D, P and T - mach number 10

- ²¹ S.C.Lin, and J.D.Teare, Rate of Ionization Behind Shock Waves in Air, II, Theoretical Interpretation, Avco Research Report 115, Sept.1962.
- ²² M.A.Biondi, Recombination Processes (Charged Particles), Defense Atomic Support Agency Reaction Rate Handbook, DASA 1948, Oct.1967, pp. 11-8 to 11-10.
- ²³ A.Q.Eschenroeder, and T.Chen, Near-Wake Ionization Behind A Sphere in Hypersonic Flight. I.Reaction Kinetics, General Motors Defense Research Labs.TR 65-01 H. Sept.,1965.
- ²⁴ A.Q.Eschenroeder, and T.Chen, Near-Wake Ionization Behind A Sphere in Hypersonic Flight. II. Influence of Flight Conditions, General Motors Defense Research Labs., TR 65-01 Q. Dec.1965.

The diffusion coefficient of NO^+ in air, denoted by \bar{D} , is about the same as that for NO in air²⁵. Consequently, using the Leonard-Jones potential, for constant pressure \bar{D} is a function of temperature only. Since $T = T(\eta)$, using the values given in Table V of reference 26, the dependence of \bar{D} on η is shown in figure 1 for sea level flight at Mach numbers 8 and 10, where the boundary layer pressures for the two cases are 4.29 and 6.00 atmospheres, respectively.

The binary diffusion coefficient for the electrons in air can be found from the approximate relation

$$\bar{D} = (\bar{M}/M)^{1/2} (\bar{T}/T) \bar{D}^+ = 2.34 \bar{D}^+, \quad (13)$$

where we have assumed $\bar{T} = T^+$.

When the turbulent Prandtl and Lewis numbers are unity, the turbulent eddy kinematic viscosity and turbulent eddy diffusion coefficients become equal²⁷. The mixing length theory of Prandtl²⁸, gives $l = Xy$ and $\overline{u'v'} = -l^2 (\frac{d\bar{u}}{dy})^2$, so that $D_T = l^2 \frac{d\bar{u}}{dy}$. With $X = 0.4$ and (2), there results for both ions and electrons,

$$D_T = 0.02 u_\delta \eta^9 / \delta. \quad (14)$$

Since $u_\delta \approx 3(10^5)$ cm/sec, for $x > 1$ cm,

$D_T > 120 \eta^{9/8}$ cm²/sec. By fig. 1, except in the neighborhood of $\eta = 0$ (that is, except in the laminar sublayer), $D_T \gg \bar{D}$. Similarly, $D_T \gg \bar{D}$ at somewhat larger X .

For small values of the ratio of the electric field to the total gas pressure, the Einstein equation $K = eD/kT$ or

$$K = 11,600 D/T \quad (15)$$

²⁵ I. Amdur and E. A. Mason, Properties of Gases at Very High Temperatures, Physics of Fluids, Vol. 1, No. 5, pp. 370-83, Sept-Oct 1958.

²⁶ I. Pollin, The Stagnation-Point Langmuir Probe in a Shock Tube--Theory and Measurements, Harry Diamond Labs, HDL TR-1103, 28 June 1963.

²⁷ W. D. Hayes, and R. F. Probstein, Hypersonic Flow Theory, pp 327-339, Academic Press Inc., 1959.

²⁸ H. Schlichting, Boundary Layer Theory, McGraw-Hill Book Co, 4th Ed., 1960, pp 477-490.

relates the mobility and binary diffusion coefficients for both electrons and ions, ref.²⁹

The y component of the ion or electron current density is defined by the equation

$$J = \pm v_D en, \quad (16)$$

($J > 0$ is in the direction toward the body surface) where the y component of the average drift velocity is

$$v_D = -v + \frac{\pm}{D} s_y / s + D_T s_y / s \pm K \phi_y \quad (17)$$

and where (+) is for ions and (-) is for electrons. Substitution of equations (16) and (17) into equations (9) and (10) and $\eta = y/\delta$ gives

$$J = \frac{en_e u s_x}{P} - \frac{We_n e}{e_e c_e} - en_e s \left(-\frac{v}{P} \right) \eta \quad (18)$$

for either ions or electrons.

Eliminating v_D in equations (16) and (17) gives

$$\frac{\pm}{s} = \frac{1}{P_T + \frac{\pm}{D}} \left[\frac{\frac{\pm}{JP_s}}{en_e} + \frac{\pm}{sv\delta} \mp K \frac{\pm}{s} \eta \right] \quad (19)$$

where the (-) and (+) signs preceding the electric mobility term are for ions and electrons, respectively.

Assuming $\phi_{\eta\eta} \gg s^2 \phi_{xx}$, Poisson's equation for the electric field is

$$\phi_{\eta\eta} = - \frac{10^{14}}{8.85} \frac{en_e s^2}{P} (s^+ - s^-) \quad (20)$$

Previously, u , T and P were made functions of η . As we have seen, equilibrium dissociation may be assumed and thereby the $\langle N \rangle$ and $\langle O \rangle$ are only functions of η . Since the pressure is constant throughout the boundary layer, $\frac{\pm}{D}$ and K are also functions of η only. By (14), at a given x , $D_T = D_T(\eta)$. The five equations (18)-(20) are explicit expressions for the derivatives $\frac{\pm}{J}$, $\frac{\pm}{s}$, $\frac{\pm}{s_x}$, ϕ_{η} in terms of $\frac{\pm}{J}$, $\frac{\pm}{s}$, $\frac{\pm}{s_x}$, ϕ_{η} . Consequently, the computation

²⁹ A. Von Engle, Ionized Gases, Oxford Univ. Press, 1955.

for \bar{J} , \bar{s} and ϕ varies with η for different x through $v=v(x,\eta)$,
 $\epsilon=\epsilon(x)$ and $\bar{s}_x = \bar{s}_x(x,\eta)$.

4. BOUNDARY CONDITIONS

The solution of equations (18), (19) and (20) requires specification of five boundary conditions in addition to initial conditions at $x = 0$. For sharp nose cones

$$\text{at } x = 0, \bar{s} = 0 \quad (21)$$

As previously stated, all ionization production occurs within a small fraction of the boundary layer adjacent to the vehicle surface. Whether a wall is catalytic or non-catalytic with respect to charged particle recombination depends on the gas-solid surface interaction, which in turn depends somewhat on the wall temperature. For the wall temperature of 1000°K assumed by Wang³⁰, experimental observations agree with the calculations obtained using the conditions $\bar{s}(0) = 0$. Similarly, we assume

$$\text{at } \eta = 0, \bar{s} = 0 \quad (22)$$

The temperatures at the edge of the boundary layer and for some distance therein are very low (see fig. 1). Except for the diffusion, this condition would give $\bar{s} = 0$ at $\eta = 1$. Calculations show that nonzero boundary conditions for \bar{s} at $\eta = 1$ wherein $\bar{s}_\eta \leq 0$ at $\eta = 1$ principally affect only the \bar{s} distributions near $\eta = 1$. Consequently, we assume

$$\text{at } \eta = 1, \bar{s} = 0 \quad (23)$$

The boundary condition for an insulated surface is $J_{\text{Net}} = \bar{J} + \bar{J} = 0$, so that $\phi_\eta(1)$ is a function of x . Including the passage of current into the wake, $\phi_\eta(1)$ is not known for a conducting surface. The value of ϕ_η near $\eta = 1$ is necessarily small because of the small values of \bar{s} near $\eta = 1$ and the electric field would appear to be small at $\eta = 1$. Accordingly, for all x , we assume

$$\text{at } \eta = 1, \phi_\eta = 0 \quad (24)$$

Thus, (24) is an approximate boundary condition for both insulated and conducting surfaces.

³⁰ K. Wang, Electron and Ion Distributions in Chemical Nonequilibrium Boundary-Layer Flows, AIAA Journal, p.316, April 1969.

In the next section, the Mach number 8 calculations show that ϕ_η is not significant in the determination of $\frac{\pm}{s}$ and $\frac{\pm}{j}$, since the $\frac{\pm}{k_0 y}$ terms are small compared to the other diffusion terms. For Mach 10, ϕ_η is small for small x , and again the effect of ϕ_η on the calculations is negligible. At larger x , the faster electron diffusion results in significant values of ϕ_η at $\eta = 0$, fig. 3(c). Upon using these values of ϕ_η for the boundary condition (24), the effect on the $\frac{\pm}{s}$ and $\frac{\pm}{j}$ distributions (not shown) was found to be limited to the neighborhood of $\eta = 1$ and did not affect the $\frac{\pm}{n}$ at $\eta = 0$ and the peak $\frac{\pm}{n}$.

Finally, in the evaluation of ϕ , we assume

$$\text{at } \eta = 1, \phi = 0 \quad (25)$$

5. NUMERICAL CALCULATIONS FOR THE ION AND ELECTRON FLOW IN THE BOUNDARY LAYER

The $\frac{\pm}{s}(x, \eta)$ in (18) can be approximated by an appropriate finite difference expression involving $\frac{\pm}{s}(x, \eta)$, $\frac{\pm}{s}(x - \Delta x, \eta)$, etc., so that the system (18)-(20) with the boundary conditions (21)-(25) ultimately reduces to solving a two-point, nonlinear boundary-value problem at each x . This was solved numerically both by integrating the differential equations and by matrix methods.³¹ As determined by reducing the step-size of the calculation intervals Δx and $\Delta \eta$ at any station x , the accuracy of any quantity was found to be within about 5 percent providing the quantity was not reduced to less than 1 percent of its maximum value. Improvement of the calculation precision requires longer computer running time.³¹

The numerical data is summarized in tables I and II and figures 2 and 3. In particular, the tables give the printout of the independent variables at typical stations $0 < x \leq 100$ as well as the contributing terms to v_D . The graphs of $\frac{\pm}{n}$ were obtained from the relation

$$\frac{\pm}{n} = n_e \frac{\pm}{s} / P \quad (26)$$

where $n_e = 6.54 (10^{10})$ and $5.63 (10^{12})$ for Mach numbers 8 and 10 and the corresponding $P = P(\eta)$ functions are given in figure 1.

³¹ A. Hausner, Ion and Electron Distributions in the Boundary Layer of Hypersonic Vehicles For Chemical Non-Equilibrium Flow - Part II: Method of Solution and Computer Program, Harry Diamond Labs., HDL-TR 1567 1971.

All functions \bar{s}^{\pm} , \bar{j}^{\pm} , and \bar{c}_n are zero at $x = 0$. The enthalpy and density profiles of the neutral gas flow result in the total ionization production occurring within a small fraction of the boundary layer in the neighborhood of the vehicle wall. For all x , the diffusion caused by concentration gradient is directed from $\eta = 0$ toward $\eta = 1$. Thus, in the neighborhood $\eta = 0$, ion-electron recombination is negligible and the ionization production remains constant for all x . The diffusion effects become significant with increasing s and therefore with increasing x . Hence, because of the diffusion, $\frac{\partial \bar{s}^{\pm}}{\partial x} < 0$ and $\bar{n} < \bar{n}_e$ in the $\eta = 0$ neighborhood.

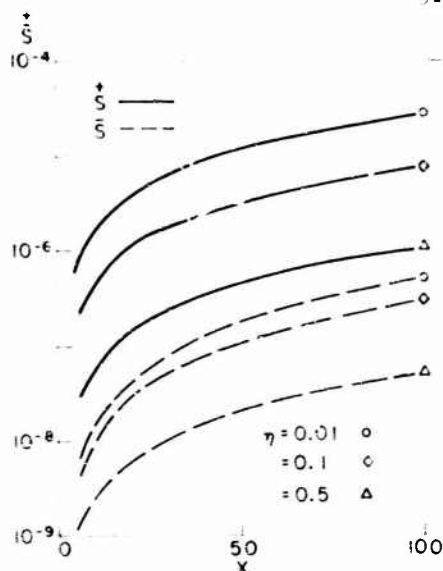


Fig. 2(a) Ion and electron densities at $\eta = 0.01, 0.1$ and 0.5 mach number 6

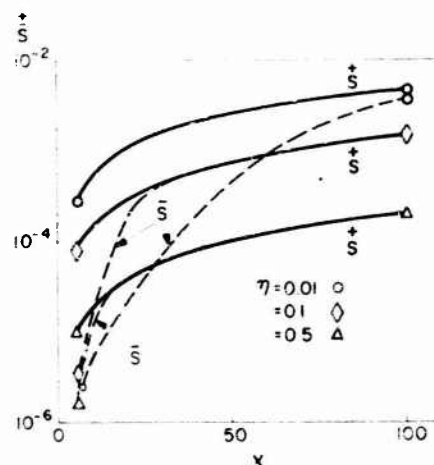


Fig. 2(b) Ion and electron densities at $\eta = 0.01, 0.1$ and 0.5 mach number 10

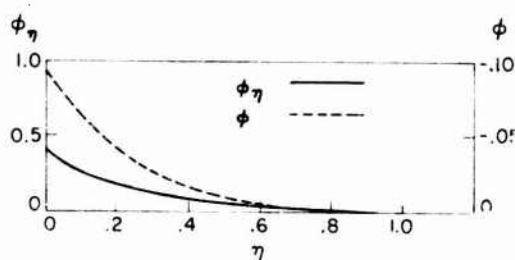


Fig. 3(a) Normalized electric field & potential at $X = 100\text{cm}$ - mach number 8

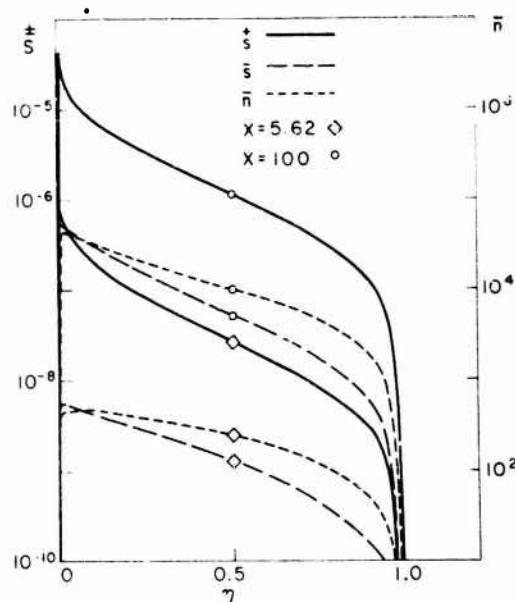


Fig. 3(b) Ion and electron densities at $X = 5.62$ and 100cm - mach number 8

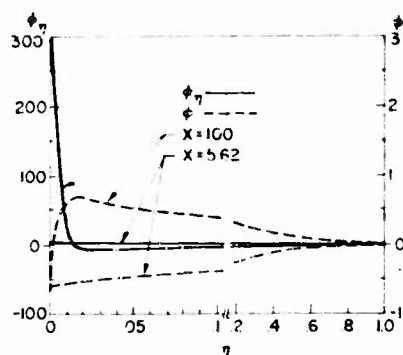


Fig. 3(c) Normalized electric field & potential at $X=5.62$ and 100cm mach number 10

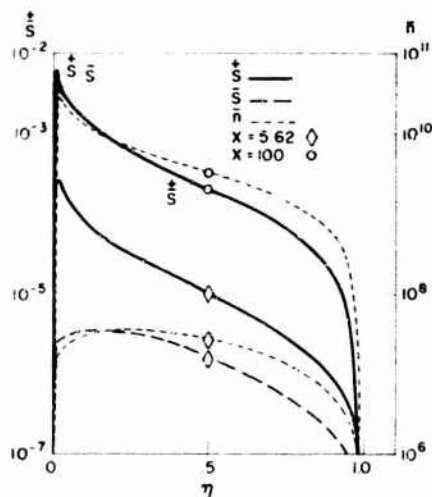


Fig. 3(d) Ion and electron densities at $X = 5.62$ and 100cm mach - mach number 10

From previous work³⁰, the u velocity is sufficiently small at $\eta \leq 10^{-4}$ to allow time for ionization equilibrium well before $x = 100$, particularly for Mach number 10. Ionization equilibrium at $\eta \leq 10^{-4}$ is denoted by $\frac{n_+}{n_-} = 1$. By figures 3(b) and 3(d), for Mach numbers 8 and 10, the diffusion reduces the peak electron density at $x = 100$ by a factor of more than 10^2 and 10^3 , respectively. On the other hand, for $x = 100$, the $\frac{n_+}{n_-}$ at $\eta > 0.1$ are much larger than those corresponding to ionization equilibrium. This occurrence is explained by the diffusion from the region $\eta < 0.1$ and the low recombination rate.

For the Mach number 10 calculations we observe the following behavior: Because of the faster electron diffusion over that of the ions, for small x , $\bar{s}(\eta) \ll \frac{n_+}{n_-}(\eta)$, fig. 2(b). As x increases, $\bar{s} \approx \frac{n_+}{n_-}$ near $\eta = 1$ and the η -region of approximate ion-electron equality progresses from $\eta = 1$ toward $\eta = 0$. Finally, at $x = 100$, $\bar{s} \approx \frac{n_+}{n_-}$ everywhere except for $\eta < 0.01$ (figs. 2(b) and 3(d)). This difference between \bar{s} and $\frac{n_+}{n_-}$ gives rise to a $\phi_{\eta} > 0$ which increases sharply near $\eta = 0$ and is a monotonically increasing function of x at $\eta = 0$ (fig. 3(c)). The values for ϕ are obtained by integration of ϕ_{η} (fig. 3(c)).

³⁰ I. Pollin, Plasma Formation in the Boundary Layer of a Sharply Pointed Hypersonic Vehicle, Harry Diamond Labs., HDL-TR-1453, June 1969.

Referring to the $\frac{1}{2}$ development with x for various η in fig. 2(b), for sufficiently large x , steady state values of $\frac{1}{2}$ will finally evolve for the Mach number 10 case with the following characteristics:

Ambipolar diffusion occurs everywhere except in the immediate neighborhood of $\eta = 0$ where $\bar{s} < \frac{1}{2}$. Because of the large $\frac{1}{2}$, the $(\frac{1}{2} - \bar{s})$ difference will give rise to a large $\phi_n > 0$ at $\eta = 0$. The peak ion-electron densities occurring in the region $\eta \leq 10^{-4}$ will be about two orders of magnitude below ionization equilibrium, whereas the ionization for $\eta > 0.1$ will greatly exceed equilibrium conditions.

The diffusion coefficients for Mach number 8 are slightly smaller than for Mach number 10. For Mach number 8, the diffusion is more effective in reducing the peak $\frac{1}{2}$ because of the slower rate of ionization production. Now, the $\frac{1}{2}$ are everywhere markedly reduced so that the contribution to v_D by the electric field resulting from charge separation is everywhere negligible, (fig. 3 (a) and table I). Hence, for Mach number 8, the electron diffusion everywhere exceeds that corresponding to ambipolar diffusion and, for all x , $\frac{1}{2} > 10 \bar{n}$ (fig. 2(a)). (If the electric field arising from the charge separation was not negligible, a counter flow diffusion would occur which would increase the peak \bar{n} and reduce the peak $\frac{1}{2}$). These effects, together with the lower n_e (by two orders of magnitude) result in reduced peak \bar{n} of about 5 to 6 orders of magnitude lower than those for Mach number 10.

6. CONCLUSIONS

The ion-electron distribution in the turbulent boundary layer has been calculated for a hypersonic vehicle consisting of a 10 degree semivertex, sharply pointed cone at Mach numbers 8 and 10 for sea level flight. Binary and turbulent eddy diffusions across the boundary layer normal to the vehicle surface act to reduce the peak $\frac{1}{2}$ whereas the electric field arising from the charge separation acts to cause ambipolar diffusion and thereby acts to increase the peak \bar{n} and decrease the peak $\frac{1}{2}$. For the cases considered, a balance between the ionization production and diffusion results in the attainment of a steady state peak electron density of about two orders of magnitude less than equilibrium ionization at Mach number 10 and a reduction of about six orders at Mach number 8. Moreover, the distance along the missile surface required to attain the steady state peak electron density in the present calculation is several times larger

than the corresponding distance to attain peak equilibrium ionization for the same flight wherein all diffusion is neglected.

The calculation procedure allows for an easy evaluation of the effect of the neutral gas enthalpy profile, boundary layer thickness, binary and eddy turbulent diffusion coefficients, etc., on the ion-electron turbulent boundary layer distributions.

The described procedure can be used to determine the ionization distributions in the turbulent boundary layer of sharply pointed vehicles for Mach numbers up to 15 at sea level and 20 at the altitude 10^5 ft. The ion mass fraction exceeds 10^{-4} at higher Mach numbers, and the electron production is no longer adequately given by reaction (1).

The assumption of the boundary conditions $s = 0$ at $x = 0$ requires a sharply pointed nose. For slightly rounded and blunt nosed vehicles, in the nose shock region, shock induced ionization governs the ion and electron distributions; however, diffusion, initially aided by recombination, will produce rapid reductions of the $\frac{1}{n}$ as the flow proceeds downstream. Consequently, for the extension to blunt nose bodies, we can assume the initial conditions to be those corresponding to equilibrium ionization behind the nose shock and proceed therefrom as before.

7. LIST OF SYMBOLS

c_j	mass fraction of component j
D	binary diffusion coefficient, cm^2/sec
D_T	turbulent eddy diffusion coefficient, cm^2/sec
e	electron charge = $1.60 (10^{-19})$ coulomb = $4.80 (10^{-10})$ esu
h	enthalpy per unit mass of mixture
H	total enthalpy per unit mass of mixture = $h + V^2$
J	y component of ion current density, Amp/cm^2
K	electric field mobility coefficient, $\text{cm}^2/\text{V-sec}$
K_f	rate constant for ion-electron formation, $\text{cm}^3/\text{ion-sec}$
K_r	rate constant for ion-electron recombination, $\text{cm}^3/\text{ion-sec}$
m	velocity profile power law coefficient = 3
M	mass, g
n	ion or electron number density, cm^{-3}
$\langle N \rangle$	nitrogen number density, atom/cm^3
$\langle O \rangle$	oxygen number density, atom/cm^3
p	pressure kg/m^2 or atmosphere
P	density ratio = ρ_e/ρ
r	radial distance of vehicle surface from axis of symmetry, cm
R	gas constant for air = $1.987 \text{ cal}/\text{mole}^\circ \text{K}$
s	mass fraction for ions or electrons = c/c_e
t	time, sec
T	absolute temperature, $^\circ \text{K}$
u	x component of neutral gas mixture velocity, cm/sec
v	y component of neutral gas mixture velocity, cm/sec
V	speed of neutral gas mixture velocity = $\sqrt{u^2 + v^2}$, cm/sec

W mass rate of formation of ions or electrons, g/sec-cm³
 x distance along meridian profile, cm
 y distance normal to the surface, cm
 Z compressibility factor = p/p_0RT ($Z = 1$ at STP)
 δ boundary layer thickness, cm
 η dimensionless boundary layer thickness = y/δ
 k Boltzmann constant = $1.38 (10^{-23})$ joule/°K
 ρ mass density, kg/m³
 ϕ electric potential, V

Subscripts

b vehicle surface
 D y component of total ion or electron velocity, cm/sec
 e recovery temperature condition ($\eta \leq 10^{-4}$)
 x partial differentiation along meridian profile
 y partial differentiation along surface normal
 δ edge of boundary layer
 η partial differentiation along dimensionless surface normal

Superscripts

- electron
 + ion

(1)

TABLE I MACH NUMBER 8

X	5.62	DELTA Z =	0.3991	ETA INTERVALS = 400	ETA	NMINUS	SPLUS	SMINUS	JPLUS	JMINUS	PHIETA	PHI	-V	KPLUS PHIV	D PLUS SV/S	D MINUS SV/S	DTPLUS SV/S	DTMINUS SV/S
0.00E-39	0.00E-39	0.00E-39	0.00E-39	3.962E-10	4.112E-10	1.036E-04	2.20E-05	0.00E-39	1.14E-02	1.00E-38	1.00E-38	1.00E-38	1.00E-38	1.00E-38	1.00E-38	1.00E-38	1.00E-38	1.00E-38
8.35E-04	1.40E-02	5.821E-07	2.736E-09	1.114E-10	1.254E-10	1.036E-04	2.19E-05	9.83E-01	1.12E-02	1.51E-06	4.17E-06	1.15E-03	1.15E-03	1.15E-03	1.15E-03	1.15E-03	1.15E-03	1.15E-03
1.75E-03	2.79E-02	7.907E-07	3.035E-09	4.297E-11	5.795E-11	1.029E-04	2.18E-05	2.27E-01	1.10E-02	4.09E-03	1.30E-06	6.98E-02	6.98E-02	6.98E-02	6.98E-02	6.98E-02	6.98E-02	6.98E-02
2.76E-03	3.31E-02	8.652E-07	4.576E-09	1.420E-11	2.915E-11	1.022E-04	2.17E-05	3.73E-01	1.08E-02	1.09E-03	5.49E-05	3.20E-02	3.20E-02	3.20E-02	3.20E-02	3.20E-02	3.20E-02	3.20E-02
3.88E-03	3.65E-02	8.869E-07	4.947E-09	1.647E-11	3.565E-11	1.018E-04	2.16E-05	5.39E-01	1.05E-02	4.66E-01	2.71E-05	2.00E-01	2.00E-01	2.00E-01	2.00E-01	2.00E-01	2.00E-01	2.00E-01
5.10E-03	3.89E-02	8.799E-07	5.173E-09	1.609E-11	3.742E-11	1.005E-04	2.15E-05	7.31E-01	1.03E-02	3.51E-01	2.41E-05	2.74E-02	2.74E-02	2.74E-02	2.74E-02	2.74E-02	2.74E-02	2.74E-02
6.52E-03	4.03E-02	8.559E-07	5.314E-09	1.672E-11	4.904E-11	9.946E-05	2.13E-05	9.45E-01	1.01E-02	5.23E-01	7.50E-04	4.64E-02	4.64E-02	4.64E-02	4.64E-02	4.64E-02	4.64E-02	4.64E-02
7.94E-03	4.17E-02	8.241E-07	5.401E-09	1.203E-11	2.673E-11	9.837E-05	2.12E-05	1.18E-01	9.94E-03	5.76E-02	3.99E-04	6.18E-02	6.18E-02	6.18E-02	6.18E-02	6.18E-02	6.18E-02	6.18E-02
9.37E-03	4.27E-02	7.882E-07	5.452E-09	1.331E-11	1.324E-11	9.721E-05	2.10E-05	1.45E-01	9.73E-03	5.78E-02	1.93E-04	8.44E-02	8.44E-02	8.44E-02	8.44E-02	8.44E-02	8.44E-02	8.44E-02
1.14E-02	4.34E-02	7.504E-07	5.477E-09	1.404E-11	5.086E-11	9.597E-05	2.08E-05	1.75E-01	9.52E-03	5.56E-02	7.25E-03	9.21E-02	9.21E-02	9.21E-02	9.21E-02	9.21E-02	9.21E-02	9.21E-02
1.44E-02	4.40E-02	7.120E-07	5.485E-09	1.446E-11	2.333E-11	9.465E-05	2.07E-05	2.09E-01	9.31E-03	5.24E-02	8.14E-03	1.04E-02	1.04E-02	1.04E-02	1.04E-02	1.04E-02	1.04E-02	1.04E-02
1.74E-02	4.46E-02	6.737E-07	5.478E-09	1.467E-11	3.072E-11	9.328E-05	2.05E-05	2.40E-01	9.04E-03	4.82E-02	8.74E-03	1.21E-03	1.21E-03	1.21E-03	1.21E-03	1.21E-03	1.21E-03	1.21E-03
2.06E-02	4.50E-02	6.361E-07	5.462E-09	1.474E-11	4.805E-11	9.180E-05	2.02E-05	3.22E-01	8.65E-03	4.46E-02	8.61E-03	1.34E-03	1.34E-03	1.34E-03	1.34E-03	1.34E-03	1.34E-03	1.34E-03
2.38E-02	4.53E-02	5.995E-07	5.439E-09	1.473E-11	5.748E-11	8.926E-05	2.00E-05	3.83E-01	8.40E-03	3.72E-02	8.41E-03	1.48E-03	1.48E-03	1.48E-03	1.48E-03	1.48E-03	1.48E-03	1.48E-03
2.70E-02	4.56E-02	5.641E-07	5.407E-09	1.467E-11	6.251E-11	8.695E-05	1.97E-05	4.39E-01	8.17E-03	3.34E-02	8.67E-03	1.63E-03	1.63E-03	1.63E-03	1.63E-03	1.63E-03	1.63E-03	1.63E-03
3.02E-02	4.62E-02	5.299E-07	5.374E-09	1.457E-11	6.509E-11	8.518E-05	1.91E-05	5.00E-01	7.92E-03	3.08E-02	8.74E-03	1.79E-03	1.79E-03	1.79E-03	1.79E-03	1.79E-03	1.79E-03	1.79E-03
3.34E-02	4.68E-02	4.969E-07	5.335E-09	1.446E-11	6.631E-11	8.332E-05	1.80E-05	5.64E-01	7.67E-03	2.80E-02	8.71E-03	1.94E-03	1.94E-03	1.94E-03	1.94E-03	1.94E-03	1.94E-03	1.94E-03
3.66E-02	4.72E-02	4.649E-07	5.290E-09	1.432E-11	6.681E-11	8.138E-05	1.88E-05	6.42E-01	7.40E-03	2.53E-02	8.85E-03	2.07E-03	2.07E-03	2.07E-03	2.07E-03	2.07E-03	2.07E-03	2.07E-03
3.98E-02	4.74E-02	4.349E-07	5.241E-09	1.418E-11	6.693E-11	7.935E-05	1.81E-05	7.24E-01	7.14E-03	2.30E-02	8.85E-03	2.20E-03	2.20E-03	2.20E-03	2.20E-03	2.20E-03	2.20E-03	2.20E-03
4.30E-02	4.74E-02	4.059E-07	5.186E-09	1.403E-11	6.686E-11	7.733E-05	1.77E-05	8.15E-01	6.87E-03	2.09E-02	8.85E-03	2.34E-03	2.34E-03	2.34E-03	2.34E-03	2.34E-03	2.34E-03	2.34E-03
4.62E-02	4.77E-02	3.774E-07	5.125E-09	1.387E-11	6.669E-11	7.523E-05	1.72E-05	9.14E-01	6.59E-03	1.89E-02	8.85E-03	2.48E-03	2.48E-03	2.48E-03	2.48E-03	2.48E-03	2.48E-03	2.48E-03
4.94E-02	4.79E-02	3.513E-07	5.058E-09	1.370E-11	6.646E-11	7.274E-05	1.68E-05	1.02E-01	6.31E-03	1.72E-02	8.85E-03	2.62E-03	2.62E-03	2.62E-03	2.62E-03	2.62E-03	2.62E-03	2.62E-03
5.26E-02	4.81E-02	3.258E-07	4.984E-09	1.352E-11	6.618E-11	7.037E-05	1.63E-05	1.14E-01	6.03E-03	1.56E-02	8.85E-03	2.76E-03	2.76E-03	2.76E-03	2.76E-03	2.76E-03	2.76E-03	2.76E-03
5.58E-02	4.82E-02	3.015E-07	4.903E-09	1.333E-11	6.585E-11	6.790E-05	1.58E-05	1.27E-01	5.74E-03	1.41E-02	8.85E-03	2.90E-03	2.90E-03	2.90E-03	2.90E-03	2.90E-03	2.90E-03	2.90E-03
5.90E-02	4.82E-02	2.784E-07	4.814E-09	1.313E-11	6.549E-11	6.536E-05	1.53E-05	1.42E-01	5.45E-03	1.28E-02	8.85E-03	3.04E-03	3.04E-03	3.04E-03	3.04E-03	3.04E-03	3.04E-03	3.04E-03
6.22E-02	4.82E-02	2.564E-07	4.716E-09	1.293E-11	6.508E-11	6.306E-05	1.48E-05	1.57E-01	5.16E-03	1.16E-02	8.85E-03	3.18E-03	3.18E-03	3.18E-03	3.18E-03	3.18E-03	3.18E-03	3.18E-03
6.54E-02	4.82E-02	2.355E-07	4.608E-09	1.271E-11	6.463E-11	6.007E-05	1.40E-05	1.75E-01	4.87E-03	1.05E-02	8.85E-03	3.32E-03	3.32E-03	3.32E-03	3.32E-03	3.32E-03	3.32E-03	3.32E-03
6.86E-02	4.80E-02	2.156E-07	4.491E-09	1.248E-11	6.414E-11	5.723E-05	1.33E-05	1.94E-01	4.58E-03	9.37E-03	8.85E-03	3.46E-03	3.46E-03	3.46E-03	3.46E-03	3.46E-03	3.46E-03	3.46E-03
7.18E-02	4.77E-02	1.968E-07	4.364E-09	1.224E-11	6.359E-11	5.438E-05	1.27E-05	2.14E-01	4.29E-03	8.68E-03	8.85E-03	3.60E-03	3.60E-03	3.60E-03	3.60E-03	3.60E-03	3.60E-03	3.60E-03
7.50E-02	4.72E-02	1.790E-07	4.225E-09	1.201E-11	6.299E-11	5.147E-05	1.19E-05	2.36E-01	3.97E-03	8.46E-03	8.85E-03	3.74E-03	3.74E-03	3.74E-03	3.74E-03	3.74E-03	3.74E-03	3.74E-03
7.82E-02	4.67E-02	1.622E-07	4.075E-09	1.170E-11	6.234E-11	4.850E-05	1.12E-05	2.60E-01	3.67E-03	7.09E-03	8.85E-03	3.88E-03	3.88E-03	3.88E-03	3.88E-03	3.88E-03	3.88E-03	3.88E-03
8.14E-02	4.63E-02	1.464E-07	3.912E-09	1.150E-11	6.163E-11	4.547E-05	1.04E-05	2.85E-01	3.37E-03	6.38E-03	8.85E-03	4.02E-03	4.02E-03	4.02E-03	4.02E-03	4.02E-03	4.02E-03	4.02E-03
8.46E-02	4.53E-02	1.316E-07	3.737E-09	1.124E-11	6.085E-11	4.240E-05	9.64E-06	3.12E-01	3.08E-03	5.74E-03	8.85E-03	4.16E-03	4.16E-03	4.16E-03	4.16E-03	4.16E-03	4.16E-03	4.16E-03
8.78E-02	4.44E-02	1.177E-07	3.550E-09	1.097E-11	6.001E-11	3.928E-05	8.82E-06	3.41E-01	2.79E-03	5.17E-03	8.85E-03	4.30E-03	4.30E-03	4.30E-03	4.30E-03	4.30E-03	4.30E-03	4.30E-03
9.10E-02	4.33E-02	1.048E-07	3.352E-09	1.069E-11	5.911E-11	3.615E-05	8.00E-06	3.71E-01	2.52E-03	4.67E-03	8.85E-03	4.44E-03	4.44E-03	4.44E-03	4.44E-03	4.44E-03	4.44E-03	4.44E-03
9.42E-02	4.20E-02	9.271E-08	3.142E-09	1.041E-11	5.815E-11	3.300E-05	7.17E-06	4.03E-01	2.24E-03	4.21E-03	8.85E-03	4.58E-03	4.58E-03	4.58E-03	4.58E-03	4.58E-03	4.58E-03	4.58E-03
9.74E-02	4.05E-02	8.154E-08	2.922E-09	1.013E-11	5.714E-11	2.984E-05	6.34E-06	4.36E-01	1.98E-03	3.34E-03	8.85E-03	4.72E-03	4.72E-03	4.72E-03	4.72E-03	4.72E-03	4.72E-03	4.72E-03
1.00E-01	3.80E-02	7.123E-08	2.694E-09	9.844E-12	5.607E-11	2.671E-05	5.51E-06	4.69E-01	1.72E-03	3.34E-03	8.85E-03	4.86E-03	4.86E-03	4.86E-03	4.86E-03	4.86E-03	4.86E-03	4.86E-03
1.00E-01	3.70E-02	6.174E-08	2.458E-09	9.560E-12	5.495E-11	2.361E-05	4.71E-06	5.03E-01	1.49E-03	3.05E-03	8.85E-03	5.00E-03	5.00E-03	5.00E-03	5.00E-03	5.00E-03	5.00E-03	5.00E-03
1.00E-01	3.49E-02	5.305E-08	2.218E-09	9.278E-12	5.381E-11	2.056E-05	3.93E-06	5.37E-01	1.25E-03	2.73E-03	8.85E-03	5.14E-03	5.14E-03	5.14E-03	5.14E-03	5.14E-03	5.14E-03	5.14E-03
1.00E-01	3.26E-02	4.512E-08	1.975E-09	8.999E-12	5.263E-11	1.759E-05	3.19E-06	5.72E-01	1.03E-03	2.47E-03	8.85E-03	5.28E-03	5.28E-03	5.28E-03	5.28E-03	5.28E-03	5.28E-03	5.28E-03
1.00E-01	3.01E-02	3.792E-08	1.732E-09	8.725E-12	5.143E-11	1.466E-05	2.50E-06	6.00E-01	8.34E-04	2.24E-03	8.85E-03	5.42E-03	5.42E-03	5.42E-03	5.42E-03	5.42E-03	5.42E-03	5.42E-03
1.00E-01	2.74E-02	3.139E-08	1.493E-09	8.460E-12	5.025E-11	1.191E-05	1.89E-06	6.33E-01	6.51E-04	2.03E-03	8.85E-03	5.56E-03	5.56E-03	5.56E-03	5.56E-03	5.56E-03	5.56E-03	5.56E-03
1.00E-01	2.49E-02	2.552E-08	1.259E-09	8.211E-12	4.910E-11	9.309E-06	1.31E-06	6.50E-01	4.86E-04	1.84E-03	8.85E-03	5.70E-03	5.70E-03	5.70E-03	5.70E-03	5.70E-03	5.70E-03	5.70E-03
1.00E-01	2.16E-02	2.027E-08	1.035E-09	7.980E-12	4.802E-11	6.907E-06	8.66E-07	6.55E-01	3.42E-04	1.69E-03	8.85E-03	5.84E-03	5.84E-03	5.84E-03	5.84E-03	5.84E-03	5.84E-03	5.84E-03
1.00E-01	1.85E-02	1.561E-08	8.212E-10	7.772E-12	4.703E-11	4.745E-06	6.62E-07	6.41E-01	2.22E-04	1.57E-03	8.85E-03	5.98E-03	5.98E-03	5.98E-03	5.98E-03	5.98E-03	5.98E-03	5.98E-03
1.00E-01	1.53E-02	1.151E-08	6.219E-10	7.591E-12	4.615E-11	2.881E-06	2.41E-07	6.02E-01	1.26E-04	1.53E-03	8.85E-03	6.12E-03	6.12E-03	6.12E-03	6.12E-03	6.12E-03	6.12E-03	6.12E-03
1.00E-01	1.19E-02	7.331E-09	4															

TABLE I MACH NUMBER 8 (Contd)

(2)

X =	22.20	DELTA Z =	0.3981	ETA INTERVALS = 400	ETA	NMINUS	SPLUS	SMINUS	JPLUS	JMINUS	PHIETA	PHI	-V	KPLUS *PHIV	O PLUS *SV/S	U MINUS *SV/S	DTPLUS *SV/S	OTMINUS *SV/S		
0.00E-39	0.00E-39	0.00E-39	0.00E-39	1.149E-09	1.232E-09	5.780E-03	-1.26E-03	0.00E-39	0.00E-39	0.00E-39	0.00E-39	0.00E-39	0.00E-39	2.15E-01	1.00E	38	1.00E	38	1.00E	38
8.45E-04	1.70E	03	4.691E-06	2.45E-08	2.949E-10	3.78E-10	5.763E-03	-1.25E-03	7.47E-01	2.09E-01	4.67E	03	1.39E	06	9.99E	02	1.26E	03		
1.75E-03	2.50E	03	5.976E-06	3.529E-08	8.970E-10	1.725E-10	5.727E-03	-1.25E-03	1.72E	00	2.04E-01	8.74E	01	4.33E	05	4.47E	02	9.40E	02	
2.76E-03	2.97E	03	6.244E-06	4.093E-08	3.505E-12	8.605E-11	5.681E-03	-1.24E-03	2.83E	00	2.00E-01	2.41E	01	1.81E	05	2.13E	01	6.82E	02	
3.08E-03	3.27E	03	6.135E-06	4.424E-08	3.671E-11	4.558E-11	5.630E-03	-1.24E-03	4.10E	00	1.95E-01	2.19E	02	8.64E	04	2.94E	02	4.75E	02	
5.10E-03	3.45E	03	5.884E-06	4.619E-08	5.719E-11	2.483E-11	5.574E-03	-1.23E-03	5.55E	00	1.91E-01	2.19E	02	4.45E	04	5.22E	02	3.55E	02	
6.45E-03	3.60E	03	5.581E-06	4.736E-08	6.840E-11	1.231E-11	5.514E-03	-1.22E-03	7.18E	00	1.87E-01	2.29E	02	2.29E	04	7.24E	02	2.44E	02	
7.94E-03	3.71E	03	5.267E-06	4.805E-08	7.476E-11	6.622E-12	5.451E-03	-1.21E-03	9.00E	00	1.84E-01	2.29E	02	1.10E	04	8.84E	02	1.52E	02	
9.57E-03	3.77E	03	4.957E-06	4.839E-08	7.346E-11	2.577E-12	5.384E-03	-1.20E-03	1.13E	01	1.80E-01	2.28E	02	4.21E	03	1.62E	03	7.24E	01	
1.14E-02	2.85E	03	4.559E-06	4.849E-08	8.053E-11	1.339E-13	5.315E-03	-1.19E-03	1.33E	01	1.76E-01	2.28E	02	2.40E	02	1.15E	03	5.18E	00	
1.34E-02	3.84E	03	4.375E-06	4.842E-08	8.167E-11	1.396E-12	5.242E-03	-1.18E-03	1.59E	01	1.72E-01	2.28E	02	2.35E	02	3.54E	03	5.71E	01	
1.55E-02	3.92E	03	4.105E-06	4.823E-08	8.216E-11	2.308E-12	5.166E-03	-1.17E-03	1.87E	01	1.68E-01	2.28E	02	3.54E	03	1.37E	03	1.13E	02	
1.79E-02	3.95E	03	3.850E-06	4.793E-08	8.223E-11	2.824E-12	5.086E-03	-1.16E-03	2.18E	01	1.64E-01	2.28E	02	4.26E	03	1.48E	03	1.55E	02	
2.06E-02	3.98E	03	3.509E-06	4.754E-08	8.244E-11	3.103E-12	5.003E-03	-1.15E-03	2.53E	01	1.59E-01	2.28E	02	4.65E	03	1.53E	03	2.14E	02	
2.35E-02	3.99E	03	3.182E-06	4.709E-08	8.168E-11	3.360E-12	4.916E-03	-1.13E-03	2.91E	01	1.55E-01	2.28E	02	4.82E	03	1.55E	03	2.63E	02	
2.67E-02	4.02E	03	3.164E-06	4.658E-08	8.123E-11	3.323E-12	4.825E-03	-1.12E-03	3.34E	01	1.51E-01	2.28E	02	4.87E	03	1.74E	03	3.15E	02	
3.02E-02	4.01E	03	2.962E-06	4.601E-08	8.070E-11	3.354E-12	4.730E-03	-1.10E-03	3.80E	01	1.47E-01	2.28E	02	4.85E	03	1.84E	03	3.70E	02	
3.41E-02	4.02E	03	2.769E-06	4.537E-08	8.011E-11	3.363E-12	4.631E-03	-1.08E-03	4.32E	01	1.42E-01	2.28E	02	4.83E	03	1.97E	03	4.39E	02	
3.84E-02	4.02E	03	2.585E-06	4.467E-08	7.948E-11	3.360E-12	4.528E-03	-1.05E-03	4.88E	01	1.37E-01	2.28E	02	4.74E	03	2.10E	03	4.98E	02	
4.31E-02	4.02E	03	2.411E-06	4.390E-08	7.882E-11	3.351E-12	4.420E-03	-1.04E-03	5.50E	01	1.33E-01	2.28E	02	4.67E	03	2.21E	03	5.73E	02	
4.82E-02	4.00E	03	2.246E-06	4.307E-08	7.811E-11	3.338E-12	4.307E-03	-1.02E-03	6.19E	01	1.28E-01	2.28E	02	4.58E	03	2.33E	03	6.58E	02	
5.39E-02	3.99E	03	2.086E-06	4.215E-08	7.731E-11	3.322E-12	4.190E-03	-0.99E-03	6.94E	01	1.22E-01	2.28E	02	4.49E	03	2.45E	03	7.55E	02	
5.92E-02	3.97E	03	1.939E-06	4.116E-08	7.657E-11	3.304E-12	4.069E-03	-0.96E-03	7.77E	01	1.18E-01	2.28E	02	4.39E	03	2.53E	03	8.50E	02	
6.71E-02	3.94E	03	1.794E-06	4.009E-08	7.574E-11	3.284E-12	3.942E-03	-0.94E-03	8.68E	01	1.13E-01	2.28E	02	4.29E	03	2.72E	03	9.50E	02	
7.47E-02	3.93E	03	1.561E-06	3.893E-08	7.487E-11	3.262E-12	3.811E-03	-0.91E-03	9.67E	01	1.07E-01	2.28E	02	4.16E	03	2.86E	03	1.11E	02	
8.31E-02	3.85E	03	1.523E-06	3.769E-08	7.396E-11	3.238E-12	3.674E-03	-0.88E-03	1.08E	02	1.02E-01	2.28E	02	4.07E	03	3.01E	03	1.26E	03	
9.23E-02	3.80E	03	1.411E-06	3.636E-08	7.300E-11	3.212E-12	3.534E-03	-0.87E-03	1.20E	02	9.70E-02	2.28E	02	3.95E	03	3.13E	03	1.43E	03	
1.02E-01	3.73E	03	1.294E-06	3.494E-08	7.200E-11	3.183E-12	3.388E-03	-0.84E-03	1.33E	02	9.16E-02	2.28E	02	3.83E	03	3.35E	03	1.61E	03	
1.14E-01	3.65E	03	1.186E-06	3.344E-08	7.095E-11	3.151E-12	3.238E-03	-0.75E-03	1.47E	02	8.63E-02	2.28E	02	3.71E	03	3.54E	03	1.82E	03	
1.26E-01	3.50E	03	1.082E-06	3.185E-08	6.908E-11	3.118E-12	3.084E-03	-0.73E-03	1.63E	02	8.09E-02	2.28E	02	3.57E	03	3.75E	03	2.05E	03	
1.39E-01	3.46E	03	9.843E-07	3.019E-08	6.876E-11	3.082E-12	2.927E-03	-0.69E-03	1.79E	02	7.53E-02	2.28E	02	3.43E	03	3.97E	03	2.30E	03	
1.54E-01	3.35E	03	8.915E-07	2.846E-08	6.741E-11	3.043E-12	2.765E-03	-0.63E-03	1.97E	02	6.97E-02	2.28E	02	3.28E	03	4.20E	03	2.59E	03	
1.71E-01	3.23E	03	8.044E-07	2.666E-08	6.641E-11	3.002E-12	2.599E-03	-0.59E-03	2.17E	02	6.42E-02	2.28E	02	3.11E	03	4.46E	03	2.90E	03	
1.89E-01	3.10E	03	7.224E-07	2.482E-08	6.518E-11	2.959E-12	2.431E-03	-0.56E-03	2.37E	02	5.88E-02	2.28E	02	2.95E	03	4.73E	03	3.23E	03	
2.09E-01	2.96E	03	6.460E-07	2.295E-08	6.393E-11	2.913E-12	2.259E-03	-0.51E-03	2.59E	02	5.35E-02	2.28E	02	2.76E	03	5.05E	03	3.60E	03	
2.30E-01	2.81E	03	5.744E-07	2.105E-08	6.265E-11	2.865E-12	2.085E-03	-0.47E-03	2.82E	02	4.84E-02	2.28E	02	2.57E	03	5.37E	03	4.01E	03	
2.55E-01	2.65E	03	5.076E-07	1.916E-08	6.135E-11	2.816E-12	1.909E-03	-0.42E-03	3.06E	02	4.33E-02	2.28E	02	2.36E	03	5.74E	03	4.46E	03	
2.81E-01	2.49E	03	4.456E-07	1.728E-08	6.004E-11	2.765E-12	1.733E-03	-0.37E-03	3.31E	02	3.83E-02	2.28E	02	2.15E	03	6.15E	03	4.96E	03	
3.10E-01	2.32E	03	3.882E-07	1.543E-08	5.872E-11	2.713E-12	1.556E-03	-0.32E-03	3.56E	02	3.35E-02	2.28E	02	1.97E	03	6.64E	03	5.52E	03	
3.42E-01	2.15E	03	3.353E-07	1.364E-08	5.741E-11	2.660E-12	1.379E-03	-0.27E-03	3.82E	02	2.88E-02	2.28E	02	1.78E	03	7.17E	03	6.15E	03	
3.78E-01	1.97E	03	2.866E-07	1.190E-08	5.611E-11	2.607E-12	1.205E-03	-0.23E-03	4.08E	02	2.44E-02	2.28E	02	1.62E	03	7.80E	03	6.97E	03	
4.17E-01	1.78E	03	2.421E-07	1.024E-08	5.482E-11	2.554E-12	1.033E-03	-0.18E-03	4.35E	02	2.03E-02	2.28E	02	1.46E	03	8.57E	03	7.71E	03	
4.59E-01	1.59E	03	2.015E-07	8.662E-09	5.358E-11	2.502E-12	8.657E-04	-0.14E-03	4.61E	02	1.54E-02	2.28E	02	1.29E	03	9.51E	03	8.73E	03	
5.06E-01	1.40E	03	1.644E-07	7.182E-09	5.240E-11	2.452E-12	7.053E-04	-0.12E-03	4.81E	02	1.29E-02	2.28E	02	1.14E	03	1.07E	04	9.97E	03	
5.58E-01	1.21E	03	1.314E-07	5.808E-09	5.131E-11	2.406E-12	5.531E-04	-0.09E-03	4.94E	02	9.63E-03	2.28E	02	1.03E	03	1.22E	04	1.15E	04	
5.15E-01	1.03E	03	1.016E-07	4.545E-09	5.032E-11	2.364E-12	4.115E-04	-0.18E-03	4.99E	02	6.80E-03	2.28E	02	0.85E	03	1.42E	04	1.37E	04	
6.78E-01	8.30E	02	7.524E-08	3.398E-09	4.945E-11	2.327E-12	2.935E-04	-0.01E-03	4.87E	02	4.41E-03	2.28E	02	0.71E	03	1.72E	04	1.57E	04	
7.48E-01	6.3E	02	5.204E-08	2.370E-09	4.874E-11	2.297E-12	1.725E-04	-0.45E-03	4.57E	02	2.51E-03	2.28E	02	0.56E	03	2.22E	04	2.16E	04	
8.24E-01	4.73E	02	3.185E-08	1.461E-09	4.81E-11	2.274E-12	8.342E-05	-0.42E-03	4.07E	02	1.13E-03	2.28E	02	0.37E	03	3.16E	04	3.12E	04	
9.08E-01	2.32E	02	1.447E-08	6.678E-10	4.789E-11	2.261E-12	2.299E-05	-0.17E-03	3.05E	02	2.83E-04	2.28E	02	0.16E	03	5.99E	04	5.96E	04	
1.00E	00	0.00E-39	0.00E-39	0.00E-39	0.00E-39	0.00E-3														

ETA	NMINUS	PLUS	SMINUS	JPLUS	JMINUS	PHIETA	PHI	-V	KPLUS *PHIY	D PLUS *SY/S	O MINUS *SY/S	OIPLUS *SY/S	OIMINUS *SY/S		
0.00E-39	0.00E-39	0.00E-39	0.00E-39	3.59E-10	4.094E-09	4.256E-01	9.50E-02	0.00E-39	4.76E	0.00E	38	1.00E	38	1.00E	39
0.03E-05	0.03E-05	0.03E-05	0.03E-05	7.50E-10	1.746E-09	4.238E-01	9.57E-02	5.05E-01	4.60E	0.973E	02	4.14E	05	6.93E	02
0.415E-03	0.415E-03	0.415E-03	0.415E-03	6.717E-11	5.618E-10	4.250E-01	9.43E-02	1.21E	0.450E	0.473E	01	1.28E	05	7.72E	01
0.276E-03	0.276E-03	0.276E-03	0.276E-03	4.504E-07	2.197E-10	4.168E-01	9.38E-02	2.10E	0.430E	0.108E	02	3.41E	02	6.35E	02
0.558E-03	0.558E-03	0.558E-03	0.558E-03	4.849E-07	3.54E-10	4.128E-01	9.34E-02	3.03E	0.429E	0.100E	02	2.48E	04	5.80E	02
0.374E-05	0.374E-05	0.374E-05	0.374E-05	5.043E-07	4.212E-10	4.085E-01	9.29E-02	4.11E	0.421E	0.124E	02	1.22E	04	7.19E	02
0.303E-05	0.303E-05	0.303E-05	0.303E-05	5.102E-07	4.582E-10	3.945E-01	9.23E-02	5.33E	0.412E	0.110E	02	5.75E	02	2.34E	02
0.470E-05	0.470E-05	0.470E-05	0.470E-05	5.219E-07	4.700E-10	3.995E-01	9.17E-02	6.65E	0.404E	0.087E	01	2.24E	03	1.03E	01
0.320E-05	0.320E-05	0.320E-05	0.320E-05	5.239E-07	4.490E-10	3.947E-01	9.11E-02	8.15E	0.395E	0.084E	01	2.33E	02	1.14E	03
0.470E-05	0.470E-05	0.470E-05	0.470E-05	5.231E-07	4.473E-10	3.898E-01	9.04E-02	9.83E	0.397E	0.273E	01	9.25E	02	1.24E	02
0.201E-05	0.201E-05	0.201E-05	0.201E-05	5.203E-07	5.006E-10	3.846E-01	8.93E-02	1.17E	0.378E	0.084E	01	1.62E	03	1.34E	03
0.470E-05	0.470E-05	0.470E-05	0.470E-05	5.158E-07	5.017E-10	3.792E-01	8.87E-02	1.38E	0.370E	0.057E	01	2.01E	03	1.45E	02
0.242E-05	0.242E-05	0.242E-05	0.242E-05	5.101E-07	5.014E-10	3.792E-01	8.79E-02	1.61E	0.361E	0.053E	01	2.20E	03	1.31E	02
0.2705E-05	0.2705E-05	0.2705E-05	0.2705E-05	5.031E-07	5.002E-10	3.677E-01	8.69E-02	1.87E	0.352E	0.045E	01	2.29E	03	1.60E	02
0.2159E-05	0.2159E-05	0.2159E-05	0.2159E-05	4.955E-07	4.945E-10	3.616E-01	8.58E-02	2.15E	0.343E	0.0396E	01	2.33E	03	1.42E	02
0.201E-05	0.201E-05	0.201E-05	0.201E-05	4.870E-07	4.943E-10	3.562E-01	8.47E-02	2.47E	0.334E	0.0354E	01	2.31E	03	1.78E	02
0.181E-05	0.181E-05	0.181E-05	0.181E-05	4.76E-07	4.938E-10	3.485E-01	8.35E-02	2.81E	0.324E	0.0316E	01	2.24E	03	1.97E	02
0.169E-05	0.169E-05	0.169E-05	0.169E-05	4.673E-07	4.911E-10	3.416E-01	8.21E-02	3.19E	0.314E	0.0242E	01	2.24E	03	1.97E	02
0.1543E-05	0.1543E-05	0.1543E-05	0.1543E-05	4.562E-07	4.883E-10	3.343E-01	8.07E-02	3.61E	0.304E	0.0207E	01	2.19E	03	2.00E	02
0.1544E-05	0.1544E-05	0.1544E-05	0.1544E-05	4.443E-07	4.852E-10	3.267E-01	7.91E-02	4.07E	0.294E	0.0206E	01	2.15E	03	2.17E	02
0.140E-05	0.140E-05	0.140E-05	0.140E-05	4.315E-07	4.820E-10	3.188E-01	7.74E-02	4.58E	0.284E	0.0203E	01	2.07E	03	2.25E	02
0.1	0.1	0.1	0.1	4.19E-07	4.786E-10	3.106E-01	7.57E-02	5.14E	0.273E	0.0143E	01	2.01E	03	2.39E	03
0.1249E-05	0.1249E-05	0.1249E-05	0.1249E-05	4.035E-07	4.750E-10	3.020E-01	7.37E-02	5.75E	0.262E	0.0104E	01	1.94E	03	2.51E	03
0.1159E-05	0.1159E-05	0.1159E-05	0.1159E-05	3.982E-07	4.712E-10	2.930E-01	7.17E-02	6.42E	0.251E	0.0084E	01	1.84E	03	2.64E	03
0.1074E-05	0.1074E-05	0.1074E-05	0.1074E-05	3.732E-07	4.672E-10	2.837E-01	6.95E-02	7.16E	0.240E	0.0053E	01	1.79E	03	2.77E	03
0.937E-06	0.937E-06	0.937E-06	0.937E-06	3.555E-07	4.630E-10	2.740E-01	6.67E-02	7.97E	0.229E	0.0012E	01	1.71E	03	2.91E	03
0.873E-06	0.873E-06	0.873E-06	0.873E-06	3.342E-07	4.586E-10	2.640E-01	6.47E-02	8.85E	0.217E	0.0009E	01	1.65E	03	3.07E	03
0.847E-06	0.847E-06	0.847E-06	0.847E-06	3.203E-07	4.539E-10	2.536E-01	6.21E-02	9.82E	0.206E	0.0008E	01	1.55E	03	3.23E	02
0.786E-06	0.786E-06	0.786E-06	0.786E-06	3.006E-07	4.491E-10	2.429E-01	5.93E-02	1.09E	0.204E	0.0008E	01	1.45E	03	3.42E	03
0.710E-06	0.710E-06	0.710E-06	0.710E-06	2.844E-07	4.441E-10	2.317E-01	5.64E-02	1.29E	0.192E	0.0007E	01	1.37E	03	3.62E	03
0.647E-06	0.647E-06	0.647E-06	0.647E-06	2.666E-07	4.389E-10	2.203E-01	5.33E-02	1.33E	0.178E	0.0007E	01	1.31E	03	3.83E	03
0.589E-06	0.589E-06	0.589E-06	0.589E-06	2.456E-07	4.33E-10	2.086E-01	5.01E-02	1.45E	0.158E	0.0005E	01	1.22E	03	4.05E	03
0.533E-06	0.533E-06	0.533E-06	0.533E-06	2.267E-07	4.270E-10	1.966E-01	4.68E-02	1.60E	0.146E	0.0005E	01	1.14E	03	4.29E	03
0.489E-06	0.489E-06	0.489E-06	0.489E-06	2.080E-07	4.212E-10	1.842E-01	4.36E-02	1.75E	0.134E	0.0003E	01	1.07E	03	4.54E	02
0.431E-06	0.431E-06	0.431E-06	0.431E-06	1.907E-07	4.152E-10	1.712E-01	3.98E-02	1.92E	0.122E	0.0003E	01	9.94E	02	4.80E	02
0.394E-06	0.394E-06	0.394E-06	0.394E-06	1.717E-07	4.101E-10	1.589E-01	3.62E-02	2.09E	0.110E	0.0002E	01	9.01E	02	5.11E	02
0.340E-06	0.340E-06	0.340E-06	0.340E-06	1.543E-07	4.040E-10	1.459E-01	3.32E-02	2.26E	0.97E	0.0001E	01	8.30E	02	5.39E	03
0.315E-06	0.315E-06	0.315E-06	0.315E-06	1.375E-07	3.971E-10	1.326E-01	2.99E-02	2.45E	0.80E	0.0001E	01	7.60E	02	5.76E	03
0.238E-06	0.238E-06	0.238E-06	0.238E-06	1.263E-07	3.911E-10	1.194E-01	2.52E-02	2.64E	0.71E	0.0001E	01	6.95E	02	6.31E	03
0.238E-06	0.238E-06	0.238E-06	0.238E-06	1.063E-07	3.851E-10	1.041E-01	2.16E-02	2.83E	0.63E	0.0001E	01	6.34E	02	6.90E	03
0.185E-06	0.185E-06	0.185E-06	0.185E-06	9.191E-08	3.788E-10	9.289E-02	1.81E-02	3.07E	0.565E	0.0001E	01	5.78E	02	7.59E	03
0.167E-06	0.167E-06	0.167E-06	0.167E-06	7.945E-08	3.726E-10	7.984E-02	1.47E-02	3.27E	0.470E	0.0001E	01	5.29E	02	8.30E	03
0.134E-06	0.134E-06	0.134E-06	0.134E-06	6.590E-08	3.666E-10	6.710E-02	1.16E-02	3.41E	0.382E	0.0001E	01	4.67E	02	9.27E	03
0.124E-06	0.124E-06	0.124E-06	0.124E-06	5.430E-08	3.608E-10	5.479E-02	9.72E-03	3.54E	0.300E	0.0001E	01	4.47E	02	1.03E	03
0.162E-07	0.162E-07	0.162E-07	0.162E-07	4.366E-08	3.555E-10	4.306E-02	8.17E-03	3.66E	0.255E	0.0001E	01	4.11E	02	1.20E	04
0.711E-07	0.711E-07	0.711E-07	0.711E-07	3.400E-08	3.507E-10	3.211E-02	4.05E-03	3.68E	0.159E	0.0001E	01	3.60E	02	1.40E	04
0.526E-07	0.526E-07	0.526E-07	0.526E-07	2.542E-08	3.449E-10	2.216E-02	2.75E-03	3.61E	0.104E	0.0001E	01	3.50E	02	1.70E	04
0.478E-07	0.478E-07	0.478E-07	0.478E-07	1.760E-08	3.400E-10	1.351E-02	1.71E-03	3.38E	0.591E	0.0001E	01	3.51E	02	2.19E	04
0.250E-07	0.250E-07	0.250E-07	0.250E-07	1.081E-08	3.404E-10	6.541E-03	3.88E-04	3.02E	0.265E	0.0001E	01	3.47E	02	3.10E	04
0.124E-07	0.124E-07	0.124E-07	0.124E-07	4.29E-09	3.339E-10	1.805E-03	5.63E-05	2.26E	0.661E	0.0001E	01	3.07E	02	3.59E	04
0.00E-39	0.00E-39	0.00E-39	0.00E-39	0.00E-39	3.335E-10	1.640E-11	0.00E-39	6.80E	0.00E	0.00E	39	1.00E	39	1.00E	39

(1)

ETA INTERVALS = 400													
ETA	MINUS	SPLUS	SMINUS	JPLUS	JMINUS	PHIETA	PHI	-V	KPLUS	C PLUS	U MINUS	OTPLUS	OTMINUS
0.000E-39	0.000E-39	0.000E-39	0.000E-39	4.514E-06	4.997E-06	2.948E	00-5.00E-01	0.00E-39	2.76E	02	1.00E	38	1.00E
1.024E-04	1.024E-04	4.219E-07	2.637E-06	2.115E-06	2.948E	00-5.97E-01	1.25E	00-5.97E-01	2.70E	02	2.48E	04	6.37E
1.675E-04	1.675E-04	7.189E-07	1.750E-06	2.232E-06	2.937E	00-5.95E-01	2.90E	00-5.95E-01	2.66E	02	8.04E	03	2.58E
2.104E-04	2.104E-04	1.245E-06	1.204E-06	1.684E-06	2.923E	00-5.92E-01	4.76E	00-5.92E-01	2.63E	02	4.14E	03	1.97E
2.348E-04	2.348E-04	1.532E-06	1.818E-07	1.298E-06	2.903E	00-5.92E-01	6.84E	00-5.92E-01	2.59E	02	2.11E	03	1.07E
2.571E-04	2.571E-04	1.780E-06	5.221E-07	9.946E-07	2.884E	00-5.945E-01	9.30E	00-5.945E-01	2.55E	02	1.33E	03	6.12E
2.649E-04	2.649E-04	1.994E-06	2.925E-07	7.580E-07	2.858E	00-5.981E-01	1.27E	00-5.981E-01	2.51E	02	4.00E	03	4.26E
2.701E-04	2.701E-04	2.181E-06	9.014E-08	5.633E-07	2.829E	00-5.977E-01	1.51E	00-5.977E-01	2.47E	01	3.04E	05	3.14E
2.745E-04	2.745E-04	2.352E-06	6.643E-08	4.003E-07	2.796E	00-5.972E-01	1.74E	00-5.972E-01	2.42E	01	1.97E	02	2.14E
2.789E-04	2.789E-04	2.494E-06	1.164E-07	2.912E-07	2.760E	00-5.967E-01	1.74E	00-5.967E-01	2.38E	03	3.27E	02	1.66E
2.833E-04	2.833E-04	2.615E-06	2.921E-07	1.823E-07	2.721E	00-5.962E-01	2.67E	00-5.962E-01	2.33E	02	3.39E	02	1.16E
2.877E-04	2.877E-04	2.741E-06	3.952E-07	1.059E-07	2.679E	00-5.956E-01	2.13E	00-5.956E-01	2.27E	02	4.37E	02	4.79E
2.921E-04	2.921E-04	2.866E-06	4.485E-07	4.802E-09	2.597E	00-5.93E-01	4.26E	00-5.93E-01	2.16E	02	4.27E	02	5.12E
2.965E-04	2.965E-04	2.931E-06	4.770E-07	2.789E-08	2.537E	00-5.935E-01	4.93E	00-5.935E-01	2.10E	02	4.10E	02	4.10E
3.009E-04	3.009E-04	3.012E-06	4.969E-07	5.233E-08	2.484E	00-5.927E-01	5.63E	00-5.927E-01	2.04E	02	3.17E	02	3.17E
3.053E-04	3.053E-04	3.094E-06	5.075E-07	6.994E-08	2.427E	00-5.919E-01	6.45E	00-5.919E-01	1.98E	02	3.02E	02	2.95E
3.097E-04	3.097E-04	3.111E-06	5.166E-07	8.199E-08	2.371E	00-5.909E-01	7.35E	00-5.909E-01	1.92E	02	3.35E	02	2.11E
3.141E-04	3.141E-04	3.155E-06	5.196E-07	9.006E-08	2.311E	00-5.904E-01	8.30E	00-5.904E-01	1.85E	02	3.38E	02	1.86E
3.185E-04	3.185E-04	3.197E-06	5.194E-07	9.533E-08	2.249E	00-5.894E-01	9.38E	00-5.894E-01	1.79E	03	2.83E	02	1.64E
3.229E-04	3.229E-04	3.235E-06	5.194E-07	9.808E-08	2.194E	00-5.877E-01	1.03E	00-5.877E-01	1.72E	02	2.66E	02	1.46E
3.273E-04	3.273E-04	3.275E-06	5.129E-07	1.007E-07	2.117E	00-5.85E-01	1.19E	00-5.85E-01	1.66E	02	2.38E	02	1.32E
3.317E-04	3.317E-04	3.314E-06	5.077E-07	1.018E-07	2.047E	00-5.82E-01	1.33E	00-5.82E-01	1.59E	02	2.17E	02	1.19E
3.361E-04	3.361E-04	3.355E-06	5.011E-07	1.022E-07	1.979E	00-5.838E-01	1.48E	00-5.838E-01	1.51E	02	1.97E	02	1.08E
3.405E-04	3.405E-04	3.402E-06	4.949E-07	1.023E-07	1.901E	00-5.823E-01	1.65E	00-5.823E-01	1.44E	03	1.79E	02	0.93E
3.449E-04	3.449E-04	3.432E-06	4.877E-07	1.022E-07	1.824E	00-5.808E-01	1.83E	00-5.808E-01	1.36E	02	1.60E	02	0.85E
3.493E-04	3.493E-04	3.467E-06	4.801E-07	1.018E-07	1.745E	00-5.791E-01	2.02E	00-5.791E-01	1.29E	02	1.47E	02	0.75E
3.537E-04	3.537E-04	3.494E-06	4.721E-07	1.014E-07	1.664E	00-5.774E-01	2.22E	00-5.774E-01	1.21E	03	1.34E	02	0.64E
3.581E-04	3.581E-04	3.524E-06	4.650E-07	1.009E-07	1.581E	00-5.756E-01	2.44E	00-5.756E-01	1.13E	02	1.22E	02	0.53E
3.625E-04	3.625E-04	3.552E-06	4.572E-07	1.002E-07	1.497E	00-5.737E-01	2.74E	00-5.737E-01	1.06E	02	1.11E	02	0.42E
3.669E-04	3.669E-04	3.580E-06	4.494E-07	9.947E-08	1.411E	00-5.719E-01	3.01E	00-5.719E-01	0.98E	02	0.90E	01	0.30E
3.713E-04	3.713E-04	3.608E-06	4.417E-07	9.871E-08	1.325E	00-5.697E-01	3.30E	00-5.697E-01	0.90E	01	0.78E	01	0.19E
3.757E-04	3.757E-04	3.636E-06	4.341E-07	9.797E-08	1.237E	00-5.674E-01	3.62E	00-5.674E-01	0.82E	01	0.65E	01	0.08E
3.801E-04	3.801E-04	3.664E-06	4.264E-07	9.716E-08	1.149E	00-5.648E-01	3.95E	00-5.648E-01	0.75E	01	0.53E	01	0.06E
3.845E-04	3.845E-04	3.692E-06	4.185E-07	9.647E-08	1.059E	00-5.624E-01	4.30E	00-5.624E-01	0.67E	01	0.41E	01	0.04E
3.889E-04	3.889E-04	3.720E-06	4.108E-07	9.571E-08	0.964E	00-5.599E-01	4.66E	00-5.599E-01	0.59E	01	0.30E	01	0.02E
3.933E-04	3.933E-04	3.748E-06	4.030E-07	9.495E-08	8.694E-01	00-5.574E-01	5.04E	00-5.574E-01	0.51E	02	0.20E	01	0.01E
3.977E-04	3.977E-04	3.776E-06	3.952E-07	9.420E-08	7.724E-01	00-5.548E-01	5.43E	00-5.548E-01	0.43E	02	0.10E	01	0.00E
4.021E-04	4.021E-04	3.804E-06	3.873E-07	9.345E-08	6.761E-01	00-5.523E-01	5.83E	00-5.523E-01	0.35E	02	0.00E	01	0.00E
4.065E-04	4.065E-04	3.832E-06	3.795E-07	9.269E-08	5.803E-01	00-5.497E-01	6.24E	00-5.497E-01	0.27E	02	0.00E	01	0.00E
4.109E-04	4.109E-04	3.860E-06	3.716E-07	9.191E-08	4.848E-01	00-5.472E-01	6.63E	00-5.472E-01	0.19E	02	0.00E	01	0.00E
4.153E-04	4.153E-04	3.888E-06	3.637E-07	9.114E-08	3.893E-01	00-5.446E-01	7.03E	00-5.446E-01	0.11E	02	0.00E	01	0.00E
4.197E-04	4.197E-04	3.916E-06	3.558E-07	9.037E-08	2.938E-01	00-5.421E-01	7.43E	00-5.421E-01	0.03E	02	0.00E	01	0.00E
4.241E-04	4.241E-04	3.944E-06	3.479E-07	8.960E-08	2.000E-01	00-5.395E-01	7.83E	00-5.395E-01	0.00E	02	0.00E	01	0.00E
4.285E-04	4.285E-04	3.972E-06	3.399E-07	8.883E-08	1.062E-01	00-5.369E-01	8.23E	00-5.369E-01	0.00E	02	0.00E	01	0.00E
4.329E-04	4.329E-04	4.000E-06	3.320E-07	8.806E-08	0.124E-01	00-5.343E-01	8.63E	00-5.343E-01	0.00E	02	0.00E	01	0.00E
4.373E-04	4.373E-04	4.028E-06	3.241E-07	8.729E-08	0.000E-01	00-5.317E-01	9.03E	00-5.317E-01	0.00E	02	0.00E	01	0.00E
4.417E-04	4.417E-04	4.056E-06	3.162E-07	8.652E-08	0.000E-01	00-5.291E-01	9.43E	00-5.291E-01	0.00E	02	0.00E	01	0.00E
4.461E-04	4.461E-04	4.084E-06	3.083E-07	8.575E-08	0.000E-01	00-5.265E-01	9.83E	00-5.265E-01	0.00E	02	0.00E	01	0.00E
4.505E-04	4.505E-04	4.112E-06	3.004E-07	8.498E-08	0.000E-01	00-5.239E-01	1.02E	00-5.239E-01	0.00E	02	0.00E	01	0.00E
4.549E-04	4.549E-04	4.140E-06	2.925E-07	8.421E-08	0.000E-01	00-5.213E-01	1.06E	00-5.213E-01	0.00E	02	0.00E	01	0.00E
4.593E-04	4.593E-04	4.168E-06	2.846E-07	8.344E-08	0.000E-01	00-5.187E-01	1.10E	00-5.187E-01	0.00E	02	0.00E	01	0.00E
4.637E-04	4.637E-04	4.196E-06	2.767E-07	8.267E-08	0.000E-01	00-5.161E-01	1.14E	00-5.161E-01	0.00E	02	0.00E	01	0.00E
4.681E-04	4.681E-04	4.224E-06	2.688E-07	8.190E-08	0.000E-01	00-5.135E-01	1.18E	00-5.135E-01	0.00E	02	0.00E	01	0.00E
4.725E-04	4.725E-04	4.252E-06	2.609E-07	8.113E-08	0.000E-01	00-5.109E-01	1.22E	00-5.109E-01	0.00E	02	0.00E	01	0.00E
4.769E-04	4.769E-04	4.280E-06	2.530E-07	8.036E-08	0.000E-01	00-5.083E-01	1.26E	00-5.083E-01	0.00E	02	0.00E	01	0.00E
4.813E-04	4.813E-04	4.308E-06	2.451E-07	7.959E-08	0.000E-01	00-5.057E-01	1.30E	00-5.057E-01	0.00E	02	0.00E	01	0.00E
4.857E-04	4.857E-04	4.336E-06	2.372E-07	7.882E-08	0.000E-01	00-5.031E-01	1.34E	00-5.031E-01	0.00E	02	0.00E	01	0.00E
4.901E-04	4.901E-04	4.364E-06	2.293E-07	7.805E-08	0.000E-01	00-5.005E-01	1.38E	00-5.005E-01	0.00E	02	0.00E	01	0.00E
4.945E-04	4.945E-04	4.392E-06	2.214E-07	7.728E-08	0.000E-01	00-4.979E-01	1.42E	00-4.979E-01	0.00E	02	0.00E	01	0.00E
4.989E-04	4.989E-04	4.420E-06	2.135E-07	7.651E-08	0.000E-01	00-4.953E-01	1.46E	00-4.953E-01	0.00E	02	0.00E	01	0.00E
5.033E-04	5.033E-04	4.448E-06	2.056E-07	7.574E-08	0.000E-01	00-4.927E-01	1.50E	00-4.927E-01	0.00E	02	0.00E	01	0.00E
5.077E-04	5.077E-04	4.476E-06	1.977E-07	7.497E-08	0.000E-01	00-4.901E-01	1.54E	00-4.901E-01	0.00E	02	0.00E	01	0.00E
5.121E-04	5.121E-04	4.504E-06	1.898E-07	7.420E-08	0.000E-01	00-4.875E-01	1.58E	00-4.875E-01	0.00E	02	0.00E	01	0.00E
5.165E-04	5.165E-04	4.532E-06	1.819E-07	7.343E-08	0.000E-01	00-4.849E-01	1.62E	00-4.849E-01	0.00E	02	0.00E	01	0.00E
5.209E-04	5.209E-04	4.560E-06	1.740E-07	7.266E-08	0.000E-01	00-4.823E-01	1.66E	00-4.823E-01	0.00E	02	0.00E	01	0.00E
5.253E-04	5.253E-04	4.588E-06	1.661E-07	7.189E-08	0.000E-01	00-4.797E-01	1.70E	00-4.797E-01	0.00E	02	0.00E	01	0.00E
5.297E-04	5.297E-04	4.616E-06	1.582E-07	7.112E-08	0.000E-01	00-4.771E-01	1.74E	00-4.771E-01	0.00E	02	0.00E	01	0.00E
5.341E-04	5.341E-04	4.644E-06	1.503E-07	7.035E-08	0.000E-01	00-4.745E-01	1.78E	00-4.745E-01	0.00E	02	0.00E	01	0.00E
5.385E-04	5.385E-04	4.672E-06	1.424E-07	6.958E-08	0.000E-01	00-4.719E-01	1.82E	00-4.719E-01	0.00E	02	0.00E	01	0.00E
5.429E-04	5.429E-04	4.700E-06	1.345E-07	6.881E-08	0.000E-01	00-4.693E-01	1.86E	00-4.693E-01	0.00E	02	0.00E	01	0.00E
5.473E-04	5.473E-04	4.728E-06	1.266E-07	6									

30